Geology, Geophysics & Environment 2024, vol. 50 (4): 357–381

Structure recognition and fluid flow potential based on well data and geological field investigations. A case study of the Istebna Beds, Silesian Unit, Carpathians

Paulina I. Krakowska-Madejska[1], Edyta Puskarczyk[2], Krzysztof Starzec[3], Jadwiga A. Jarzyna[4], Marek Stadtmüller[5]

[1] *AGH University of Krakow, Faculty of Geology, Geophysics and Environmental Protection, Department of Geophysics, Krakow, Poland, ORCID ID: 0000-0002-8261-4350, e-mail: krakow@agh.edu.pl (corresponding author)*
[2] *AGH University of Krakow, Faculty of Geology, Geophysics and Environmental Protection, Department of Geophysics, Krakow, Poland, ORCID ID: 0000-0001-5277-0507*
[3] *AGH University of Krakow, Faculty of Geology Geophysics and Environmental Protection, Department of General Geology and Geotourism, Krakow, Poland, ORCID ID: 0000-0001-6538-5296*
[4] *AGH University of Krakow, Faculty of Geology, Geophysics and Environmental Protection, Department of Geophysics, Krakow, Poland, ORCID ID: 0000-0002-1803-8643*
[5] *Oil and Gas Institute – National Research Institute, Krakow, Poland, ORCID ID: 0000-0001-9684-933X*

Received: 18 March 2024; accepted: 24 September 2024; first published online: 6 December 2024

Abstract: Facies were recognized based on the results of well logging data, using these measurements and conducting a comprehensive interpretation. This was done by first using shaliness (volume of shale) as the main parameter for a geological profile division into petrophysical lithofacies before secondly calculating Flow Zone Index (FZI), utilizing porosity and permeability estimated from well logging interpretation and defining Rock Types on the basis of FZI frequency distributions. FZIs were also determined according to porosity and permeability from laboratory measurements whenever the results were available. Descriptions of cores and cuttings together with the results of geological field investigations were the basis for lithofacies determination. Maps of average porosity, permeability, and FZI values were constructed for the study area. Three types of facies data and maps of reservoir parameters were used to support the recognition of geological structures and their assessment of potential for fluid movement in the rock formation. The facies analyses were performed on the example of the Istebna Beds of the Silesian Unit in the Carpathians.

***Keywords*:** well logging measurements and interpretation, cores and cuttings, geological field investigations, Flow Zone Index, Rock Types, Istebna Beds, Carpathians

INTRODUCTION

Combining the results of geological field investigations, data obtained in wells by logging measurements, descriptions and analyses on cores and cuttings is a difficult task due to the diverse resolution of the information coming from these sources. However, it is extremely important since it allows the continuous results of well logging to be combined with point-source measurements on rock material, collected both from wells and from outcrops. Petrophysicists are aware of the

differences in measurement conditions between wells and in the laboratory, as well as the impact of well conditions on the determined parameters, despite the measures taken to eliminate the adverse effect of mud in the well and the destruction of the well walls. The incentive to undertake the work on combining information from different sources is always its potential to extend the actual values (measured in the field or on the core) to the entire well profile and, more broadly, decipher the three-dimensional geological structure, based on the correct connection of information from many wells. The combination of information concerns both qualitative features (structure, texture, color, grain size, and degree of rock sorting) and parameters expressed numerically (thickness, volume of mineral components, porosity, and permeability).

In this study, the focus was on facies, understood as petrophysical lithofacies (f_sandstone, f_mudstone, f_claystone) and determined on the basis of the dominance of specific mineral or lithological components, above all shaliness, essentially influencing the volume of the other components (sandstone, mudstone, claystone, possibly carbonate), provisionally named interpretive facies (Stadtmüller et al. 2021–2022). Lithofacies were also described, determined only according to geological criteria on the basis of core descriptions and cuttings in combination with facies defined on the basis of field investigations and geological knowledge. The subject of this work was also the Flow Zone Index (FZI) (Amaefule et al. 1993, Prasad 1999, 2003, Mahjour et al. 2015, Al-Askari & Kamal 2017), the frequency distributions of which, calculated in specific geological divisions, became the basis for the classification of Rock Types (Al-Jawad & Saleh 2020, Houshmand et al. 2022, Mahmoud et al. 2023, Saadat & Rahimpour-Bonab 2023). The FZI was calculated primarily from reservoir parameters interpreted from well logs but also from the results of porosity and permeability tests on samples cut from cores. The juxtaposition of petrophysical lithofacies, lithofacies, and Rock Types contributed to a more accurate division of the well profiles into reservoir, sealing and source layers and the separation of beds characterized by enhanced media flow capacities.

On the basis of porosity (PHI) resulting from the comprehensive interpretation of well logs (Alberty & Hashmy 1984, Doveton & Prensky 1992, Jarzyna et al. 2000), permeability (K) estimated on the basis of porosity (Zawisza 1993) and FZI calculated on their basis, maps of variability of these parameters in the study area were drawn for the Istebna Beds. Zones with the best properties for hydrocarbon migration and accumulation were depicted on the maps, as well as a comparison of mapped zones of reservoir parameters and geological structures.

The novelty of the presented solution is based on the petrophysical interpretation of well logs, calibrated with laboratory results used for lithology recognition, together with FZI parameters enabling a combined projection of the reservoir capacity of the rock. Point and direct geological information from cores, cuttings, and direct field geological investigations increase the chances of correct facies differentiation and the proper delineation of reservoirs.

GEOLOGICAL STRUCTURE OF THE STUDY AREA

The study area is situated in the middle part of the Polish Outer Carpathians that are composed of a stack of nappes containing up to 6 km of Upper Jurassic-Neogene sedimentary sequences. Investigations included rocks belonging to the Silesian Unit that in Polish part of the Carpathians stretches from the Beskid Śląski to the Bieszczady Mountains. From the south, the unit is covered by the Magura and Dukla units and to the north is thrust onto the Sub-Silesian and Skole units (Fig. 1). The sedimentary succession of the Silesian Unit is composed of rocks ranging from the age from the Upper Jurassic to the Miocene (e.g. Książkiewicz 1977, Oszczypko et al. 2008). The lowermost part of the succession consists of the Upper Jurassic to Lower Cretaceous formations (i.e. Cieszyn, Hradiste, Verovice and Lgota formations), the middle part includes the Godula and Istebna Beds of Upper Cretaceous to Paleocene age, which are followed by the Eocene Variegated Shales with the Ciężkowice Sandstone and the Oligocene Menilite and Krosno Beds (e.g. Paul et al. 1996) (Fig. 2).

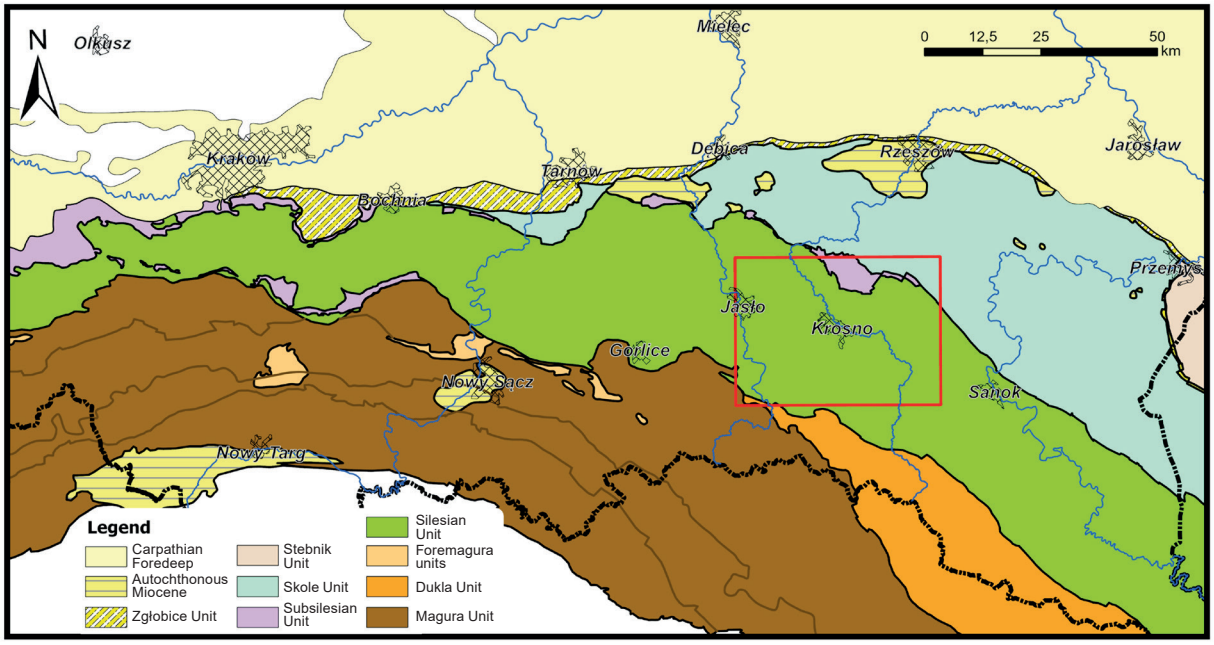

Fig. 1. *Location of the studied area (red rectangular) on the geological sketch of the Polish Outer Carpathians*

Within the study area, the Silesian Unit is composed of several thrust sheets striking in NW-SE direction. The Istebna Beds from more than a dozen wells located in different thrust sheets were the subject of this study. The list of the wells is included in the table in the final part of the article, while the maps of the reservoir parameters, constructed on the basis of the obtained results, are described to avoid repetition. From the north, these are as follows: the Glinik syncline with the Si-1 well occurring in the axis of this syncline, the Potok – Krościenko anticline pierced by the wells no. J-24, J-35, J-36 in its axial zone, and the wells no. So-17, So-18 and So-29, occurring on the southern limb of the anticline, the Bóbrka – Rogi anticline with two wells: R-1, R-2 and the most southern structural component, i.e. the Iwonicz-Zdrój (Draganowa) – Rudawka Rymanowska anticline with the wells: Dr-1 and Du-1. The following sheets of the Detailed Geological Map of Poland (DGMP): Frysztak (Birkenmajer-Szymakowska et al. 2009), Jedlicze (Szymakowska & Wójcik 1992a, 1992b), Krosno (Piotrowska & Wasiluk 2009a, 2009b), Nowy Żmigród (Jankowski et al. 2012), Rymanów (Wdowiarz et al. 1991a, 1991b), published interpretations of geological, well logging and seismic data (Wdowiarz 1950, Kruczek 1956, 1968, 1999, Unrug 1963, Mitura & Birecki 1966, Konarski 1980, Kępińska 1986, Baszkiewicz et al. 2001, Strzeboński 2005, 2015, Dziadzio 2006) and a brief characterization of the structural elements is presented based on the surface data. Well data were also investigated, available from the Polish Geological Institute – National Research Institute portal and the own research materials of the authors. More detailed considerations were carried out on data from the Potok – Krościenko anticline, in particular from the J-36 and M-6 wells.

The Istebna Beds represent a prominent component of the sequence of the Silesian Unit, up to 1500 m in thickness, occupying the position above the sandstone-shale Godula Beds and below the red shales of the Variegated Shales. The Beds are divided into two members – the Lower and Upper Istebna Beds (Fig. 2). The first member includes mostly thick-bedded sandstone layers, while the latter is divided into three divisions, i.e. the Lower Istebna Shale, Upper Istebna Sandstone and Upper Istebna Shale reflecting the dominant rock inventory of the respective division.

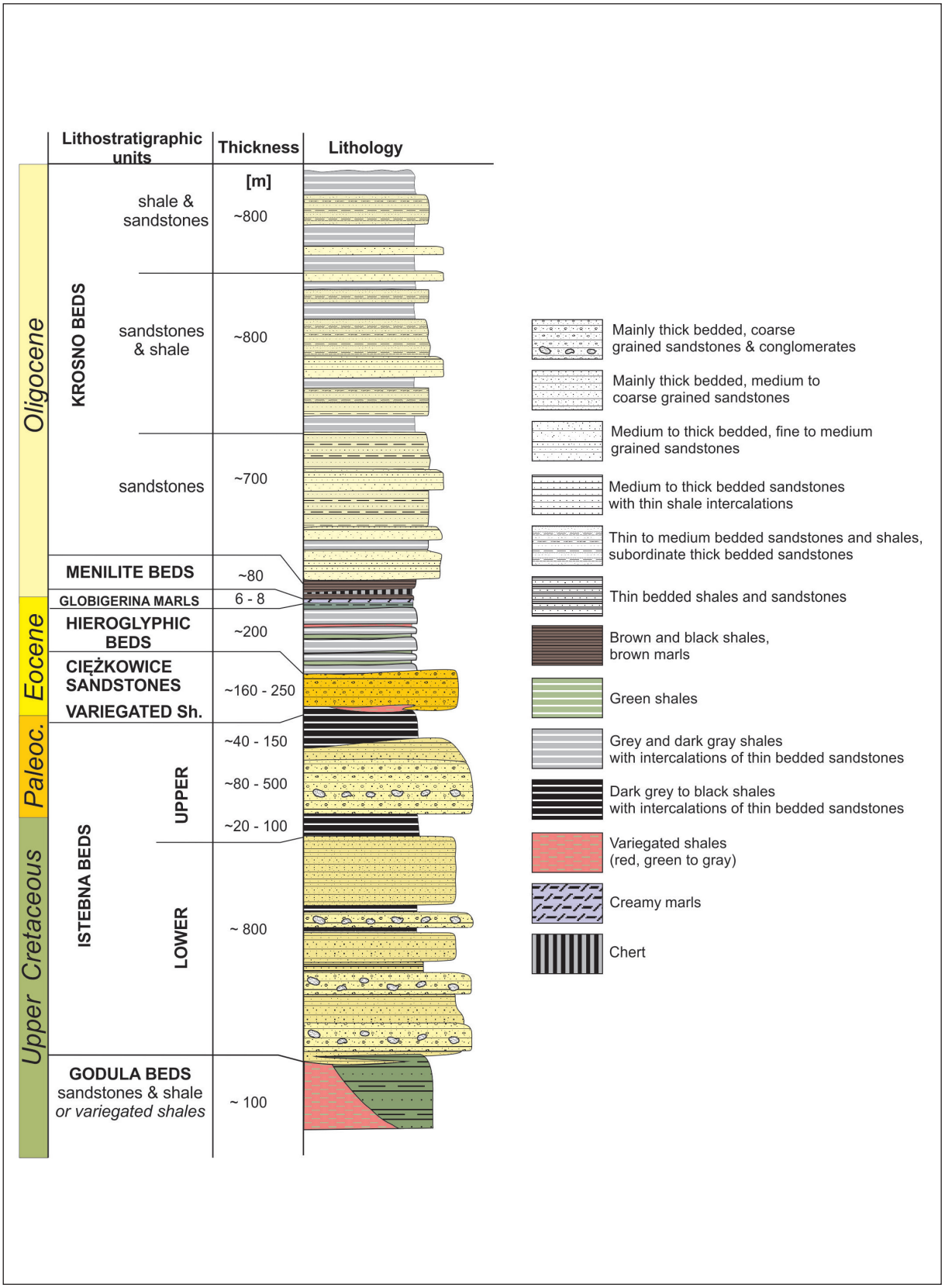

Fig. 2. *Lithostratigraphic scheme of the Upper Cretaceous to Oligocene sequence of the Silesian Unit in the study area showing the position of the Istebna Beds and their facial character*

Lithologically thick-bedded sandstones of the Upper Istebna are similar to the sandstone layers of the lower member, therefore in case of absence of the shale horizon between them, caused either by the real absence of such shales in the sequence of the Istebna Beds, or by the poor condition of the exposures, it is impossible to divide the lower and upper members, and therefore on some sheets of the DGMP these two members are presented as undivided Istebna Beds.

Lower Istebna Beds

The dominant lithology includes coarse and very coarse, thick-bedded sandstones and conglomerates, subordinate sandy shales or shale-sandstone packages, and intervals of paraconglomerates up to several meters thick. The latter type of rocks is an important element of the succession of both the Lower Istebna Beds and the Upper Istebna Sandstones, which from a genetic point of view represent cohesive debrites (Strzeboński 2005). Their thicknesses often reach several meters. They are composed of a mixture of silty-sandstone matrix and material of gravel fraction, forming a dispersed grain framework. Stratigraphically, in the study area the Lower Istebna Beds overlie the Godula Beds, while from above they are covered by the Lower Istebna Shale. Within the study area, the thickness of these layers reaches about 800 m. The Lower Istebna Beds are dated to the Late Cretaceous (Early Senonian).

Lower Istebna Shales

This member is composed of clayey to sandy shales, dark grey to black in color, subordinately interbedded by thin layers of very fine-grained sandstones, less frequently by siderite. The shales are rich in organic matter and are also characterized by a high content of muscovite. More sandy layers show a brittle character. In some layers the shales resemble heteroliths, i.e. siltstones with lenses, or laminae of sand. Stratigraphically, the Lower Istebna Shales separates two sandstone complexes – the Lower and Upper Istebna Beds. This member forms a relatively thin strata with a thickness of 40–150 m.

Upper Istebna Sandstones

This member is dominated by thick-bedded, usually coarse-grained sandstones with a carbonate cement. Sandstones are sometimes interbedded by thick layers of conglomerates and paraconglomerates (debrites). Lithologically, the member is almost identical to that of the Lower Istebna Beds, the main differences lie in the presence of carbonate-cemented sandstones and a smaller proportion of debrites. Moreover, the thickness of this member is smaller and variable, falls within a range of 80–500 m. The member is overlined by the Upper Istebna Shales, although these shales do not always form a continuous horizon and then the sandstones are directly covered by the Hieroglyphic Beds. The age of the Upper Sandstone member of the Istebna Beds is estimated at the Paleocene.

Upper Istebna Shale

The uppermost part of the Istebna Beds is composed of clayey to sandy shales, with abundant muscovite and plant detritus. Subordinately shales are interlayered by thin sandstones. Thin layers of variegated shales occasionally appear, which are absent in the lower division of the Istebna Shale. The thickness of the Upper Istebna Shale ranges in 20–100 m. This member is an overburden of the Upper Istebna Sandstones and is covered by the Variegated Shales or Hieroglyphic Beds. Together with the Upper Istebna Sandstones, this member is included in the Paleocene.

Structural characteristics of the Potok – Krościenko anticline

Wells J-36 and M-6 are located on the axial zone of the Potok – Krościenko anticline, which has the character of a steep fold with an axis slightly inclined toward the NE (Fig. 3). This fold is subjected to undulations and its axial zone plunges towards the NW. Well So-17 and So-29 are located on the southern part of the western end of the fold.

Along the axial zone of the anticline, the Menilite Beds and Variegated Shales and Hieroglyphic Beds are outcropped at the surface.

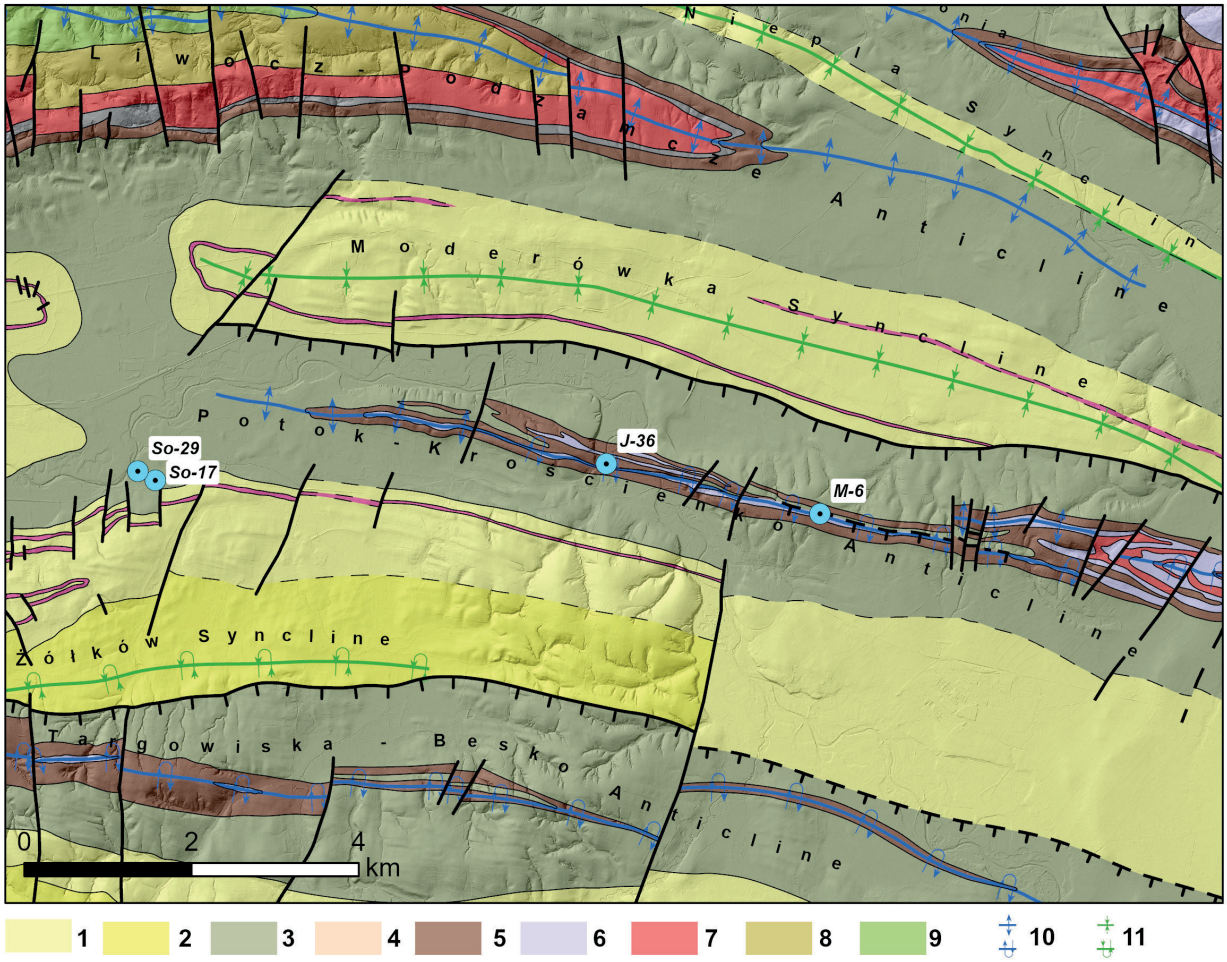

Fig. 3. *Geologic map of the middle part of the study area with the location of J-36, M-6, So-29 and So-17 wells; explanation of symbols: 1–3 – Krosno Beds (1 – shale and sandstone, 2 – sandstone and shale, 3 – thick-bedded sandstone), 4 – Transitional Beds, 5 – Menilite Beds, 6 – Hieroglyphic Beds, 7 – Variegated Shales and Ciężkowice Sandstones, 8, 9 – Istebna Beds (8 – Upper, 9 – Lower), 10 – axis of anticline (symmetrical, overturned), 11 – axis of syncline (symmetrical, overturned) (map acc. to Starzec 2016 based on Szymakowska & Wójcik 1981)*

In the area of the greatest uplift of the fold (in the Krosno region), the Ciężkowice Sandstones additionally appear between the Variegated Shales, while rocks older than the Eocene are not exposed. However, they have only been drilled in numerous wells distributed along the continuity of the fold to the west, the results of which indicate the relatively complex structure of the axial zone – the core of the fold has a chimney-like structure, which is associated with intensive foliation of the Eocene-Oligocene strata to considerable depths, below which the fold is gradually flattened, and in its core appear older formations of the Istebna Beds. Depending on the location of the well, the Istebna Beds were reached at different depths, e.g. in the well J-36 top of the Beds is at a depth of 1020 m, in M-6 at a depth of 1,090 m, while in the So wells area the depth of the Istebna layers reaches about 1,300 m. None of the aforementioned wells pierced the bottom of the Istebna Beds because they dip at relatively steep angles, making any estimate of their actual thickness in this structural element very difficult as a result.

RESEARCH METHODOLOGY, STUDY MATERIAL, AND RESULTS

The results of the reinterpretation of the well logging, as well as descriptions of cores and drill cuttings sourced from the well documentation

provided by Polish Oil and Gas Company (PGNiG S.A.) were used under the INNKARP (2019–2023) project financed in the frame of Smart Growth Operational Programme by the National Center for Research and Development and POGC, Warsaw, Poland (Jarzyna et al. 2021–2022, Stadtmüller et al. 2021–2022).

Petrophysical lithofacies determination

Petrophysical lithofacies, tentatively named interpretive facies, were determined (Stadtmüller et al. 2022) as a result of combining geological information and amount of clay (Vcl), as well as the volume of the sandstone component (Vsand) interpreted from well logging. These included

- the sandstone facies: f_sandstone, where Vcl < 35%,
- the mudstone facies: f_mudstone, where 35% < Vcl < 65%,
- the claystone facies: f_claystone, where Vcl > 65%.

Based on these, profiles of the wells were divided into parts with reservoir, seal and source rock characteristics. Carbonate facies (Vlime) was separated in the profiles of some wells, for a more precise definition of sealing zones, based on the carbonate content: f_lime, where Vlime > 30%. The obtained results of the division into petrophysical lithofacies are always presented on the initial tracks of the graphs.

Lithofacies from field reconnaissance

Based on field study, several facies in the Istebna Beds can be determined applying the criteria of lithology and layer thickness. The term lithofacies is used to distinguish them from the petrophysical lithofacies determined on the basis of the well logging data. In the case of thick-bedded formations, individual lithofacies are limited to single layers, while in thin-bedded formations, a single lithofacies is formed by an assemblage of two or more lithologies (e.g., sandstone and shale) and is distinguished based on the proportion of individual components. Individual lithofacies within the profile of the Istebna Beds can either form packages of different thicknesses (from several to several tens of meters) or can occur alternately. The main characteristics of the lithofacies of the Istebna Beds are shown in Table 1 and some field examples of these lithofacies are illustrated in Figure 4.

Table 1
Characteristics of the lithofacies in the Istebna Beds

Lithofacies	Description
I, thick-bedded conglomerates	fine- to medium-graveled conglomerates in layers or irregular lenses of about 2–3 m in thickness, sometimes thicker
II, thick-bedded paraconglomerates (debrites)	very thick-bedded layers, from 1–2 m to more than 20 m, composed of a mixture of silty-sandy matrix and dispersed material of gravel fraction
III, thick-bedded conglomeratic sandstones	coarse-grained sandstones with gravel material, mostly thick-bedded, usually between 0.5 and 2 m in thickness, occurring in packages of total thickness of several meters
IV, coarse- to medium-grained sandstones	similarly, as in the previous facies, layers are 0.5–2.0 m thick and are usually separated by very thin silty shales
V, fine- to medium-grained sandstones and shales	sandstone-shale couplets usually in packages of several meters thick, with predominance of sandstone layers ranging from thin- to thick-bedded, accompanied by thin shale layers
VI, sandstones, shales and marls	alternation of shales, marls and sandstones, shales and marls of thin to medium thickness (about 10–30 cm)
VII, thin-bedded shales and sandstones	thin- and medium-bedded shales, interlayered with very thin layers of fine-grained sandstones up to a few centimeters in thickness
VIII, shales and mudstones	silty, sometimes sandy shales, usually thin-bedded (a few or several centimeters thick), occurring in packages with a thickness of up to several meters

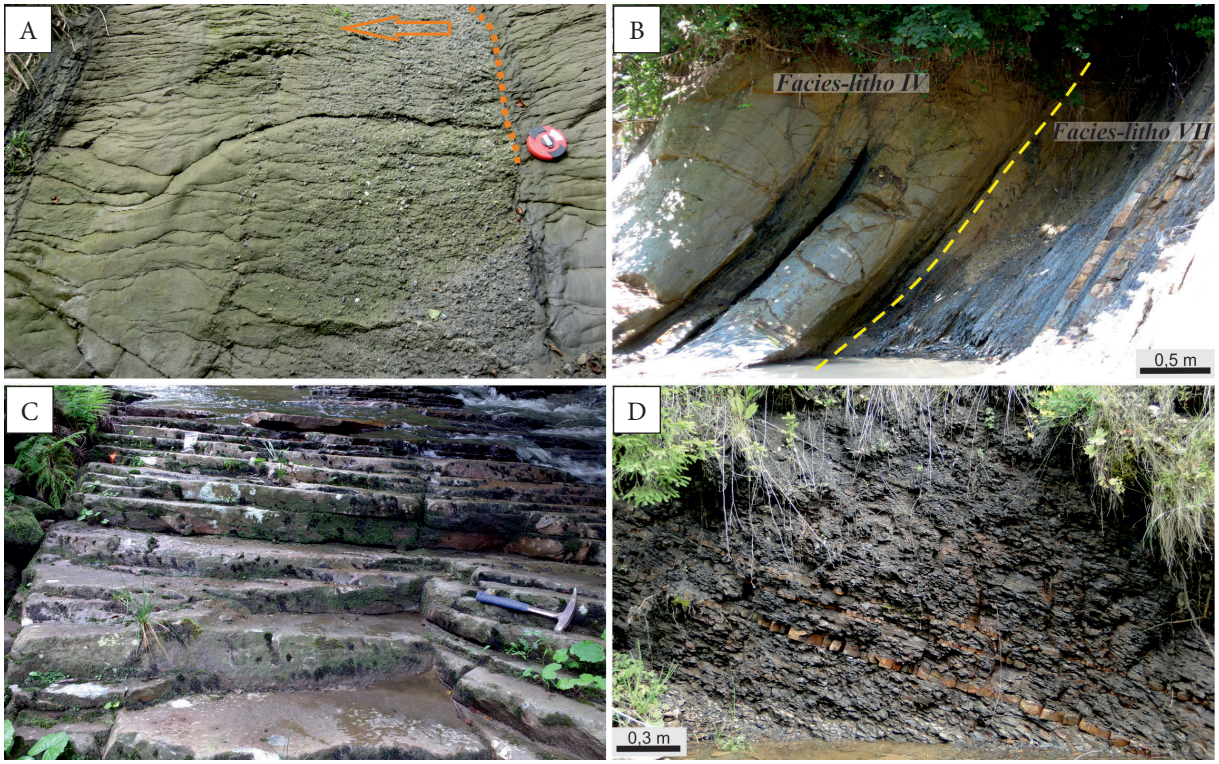

Fig. 4. *Examples of rocks in outcrops representing different lithofacies within succession of the Istebna Beds: A) thick-bedded sandstone showing normal grading from coarse grains with pebbles to medium fraction – lithofacies III; B) contact between package of thin-bedded shales and sandstone – lithofacies VII – and thick layers of coarse- to medium-grained sandstones – lithofacies IV; C) package of thin and medium-bedded, find and medium-grained sandstones – lithofacies V; D) package of very thin-bedded shales intercalated with thin layers of orange-colored siderite – lithofacies VIII*

FZI and Rock Types in well profiles based on the results of reinterpretation of well logging

FZI is a qualitative and quantitative indicator of zones with the fluid flow ability. The basis for calculating the FZI index is Equation (1):

$$\mathrm{FZI} = 0.0314 \cdot \left[\frac{\sqrt{\frac{K}{F}}}{\frac{F}{1-F}} \right] \tag{1}$$

where: K – permeability [mD], F – porosity [dec].

FZI values were calculated for the laboratory and well logging data sets in the studied wells based on the available values of effective porosity from various laboratory tests and the total porosity from interpretation of the well logs, as well as the permeability measured directly on the samples or estimated from the results of the well logging interpretation. In the figures presenting the results, FZIs from laboratory measurements are included to highlight the information acquired in surveys with different levels of detail. Frequency histograms of FZIs were the basis for determining Rock Types, separate groups with the similar data characteristic, e.g. physical rock properties.

Research material and results in J-36 well

Due to the lack of outcrops of the Istebna Beds along the Potok – Krościenko fold, the lithofacies were determined only on the well data (descriptions of cuttings and cores) but considering the characteristics of the lithofacies determined in the field (Table 2). In well J-36, the Lower Istebna Beds begin at the depth of 1637 m, and up to the final depth of the well (2322 m) several sandstone intervals (most likely representing lithofacies III and IV, i.e. conglomeratic-sandstone and coarse- and medium-grained

sandstone) were identified in this member, which are interbedded by shale or shale-sandstone intervals (lithofacies VII and VIII) (Table 2). According to the well documentation (Plezia 1995), several horizons with good reservoir properties, often saturated with hydrocarbons (labeled A–E in Table 2), were identified in the sandstone intervals of the Istebna Beds.

Table 2
Division of the Istebna Beds into lithofacies in the J-36 well based on descriptions of cores and drill cuttings

Lithostratigraphy (top and bottom) acc. to the well documentation	**Top [m]**	**Bottom [m]**	**Lithological divisions according to the well data**	**No. of lithofacies**	**Lithofacies**
Upper Istebna Shales (1020–1042 m)	1020	1046	–	VII	thin-bedded shales and sandstones
Upper Istebna Sandstones (1042–1462 m)	1042	1200	sandstones, horizon A	V	fine- to medium-grained sandstones and shales
	1200	1253	shales with sandstone layers	VII	thin-bedded shales and sandstones
	1253	1462	sandstones, horizon B	V	fine- to medium-grained sandstones and shales
Lower Istebna Shales (1462–1637 m)	1462	1637	–	VIII	shales and mudstones
Lower Istebna Beds (1637–1665 m)	1637	1665	sandstones, horizon C1	IV	coarse- to medium-grained sandstones
	1665	1669	shales	VIII	shales and mudstones
	1669	1705	sandstones, horizon C2	IV	coarse- to medium-grained sandstones
	1705	1735	shales	VIII	shales and mudstones
	1735	1795	sandstones, horizon C3	IV	coarse- to medium-grained sandstones
	1795	1807	shales	VIII	shales and mudstones
	1807	1834	sandstones, horizon C4	IV	coarse- to medium-grained sandstones
	1834	1875	shales	VIII	shales and mudstones
	1875	1997	sandstones, horizon C5	IV	coarse- to medium-grained sandstones
	1997	2030	shales	VIII	shales and mudstones
	2030	2156	sandstones, horizon D	V	fine- to medium-grained sandstones and shales
	2156	2222	sandstones overlain by dark gray shale	V	fine- to medium-grained sandstones and shales
	2222	2315	fine and coarse-grained sandstones, horizon E	IV	coarse- to medium-grained sandstones
	2315	2335	grey shales with sandstone layers	VII	thin-bedded shales and sandstones

The data from J-36 well indicate that in the case of the Potok – Krościenko fold, the Lower Istebna Beds show much greater variation in terms of the ratio of sandstone to shale facies compared to other regions, such as the Glinik syncline. It should be noted, however, that debrite, especially if it is characterized by a highly dispersed grain framework and a high proportion of clay fraction in the matrix, can give a record on the intensity curves of natural gamma radioactivity (GR) similar to that of mudstone, and will be difficult to identify in cutting samples. Therefore, it is possible that some of the intervals identified in the well as shales may represent debrite facies.

FZI histograms in the J-36 well were divided in three ways to define Rock Types. The two first subdivisions included four classes, two last – three classes (Table 3). The first subdivision (I) includes the same classes as in other wells. The second subdivision (II) yields a result that followed a normal distribution (Fig. 5), while the third one (III) maintained a similar abundance in classes. The last subdivision (IV) is related to the FZI calculated from the laboratory results.

It can be seen that there is little data in the lowest class. Two classes between 0.5 and 2 FZI ranked a total of 87% of the data (Fig. 5A). The classes between 0.73 and 2.19 FZI have a total of 78% of the data (Fig. 5B). There is also relatively little data in the highest class. The higher the FZI value, the higher Rock Type and the better the reservoir properties.

Table 3
FZI subdivisions into classes in J-36 well

Subdivision	Class 1	Class 2	Class 3	Class 4
I	FZI < 0.50	0.50 < FZI < 1.00	1.00 < FZI < 2.00	2.00 < FZI < 4.00
II	FZI < 0.73	0.73 < FZI < 1.46	1.46 < FZI < 2.19	FZI > 2.19
III	FZI < 1.00	1.00 < FZI < 1.50	FZI > 1.50	–
IV	FZI < 0.39	0.39 < FZI < 0.63	FZI > 0.63	–

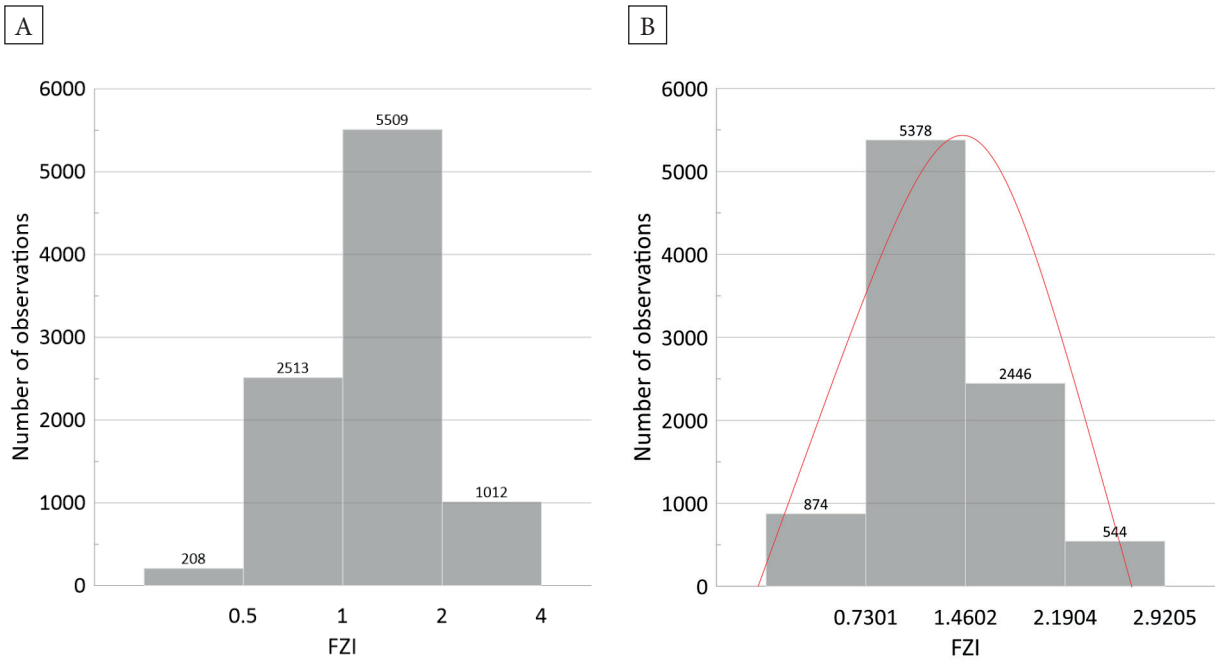

Fig. 5. *FZI histograms for the Istebna Beds in J-36 well by classes according to the subdivisions in Table 3. The first subdivision (I) on the left (A) includes the same classes, as in other wells, while the second subdivision (II) on the right (B) yields a result that followed a normal distribution of the data*

The facies determined by different methods in the interval of the Istebna Beds (Upper Istebna Beds: 1020–1462 m, Lower Istebna Beds: 1462–2335 m) are summarized in Figure 6. The sandstone, mudstone and claystone petrophysical lithofacies: f_sandstone, f_mudstone and f_claystone, determined by Stadtmüller et al. (2021–2022) are shown in red, in paths 4, 5 and 6.

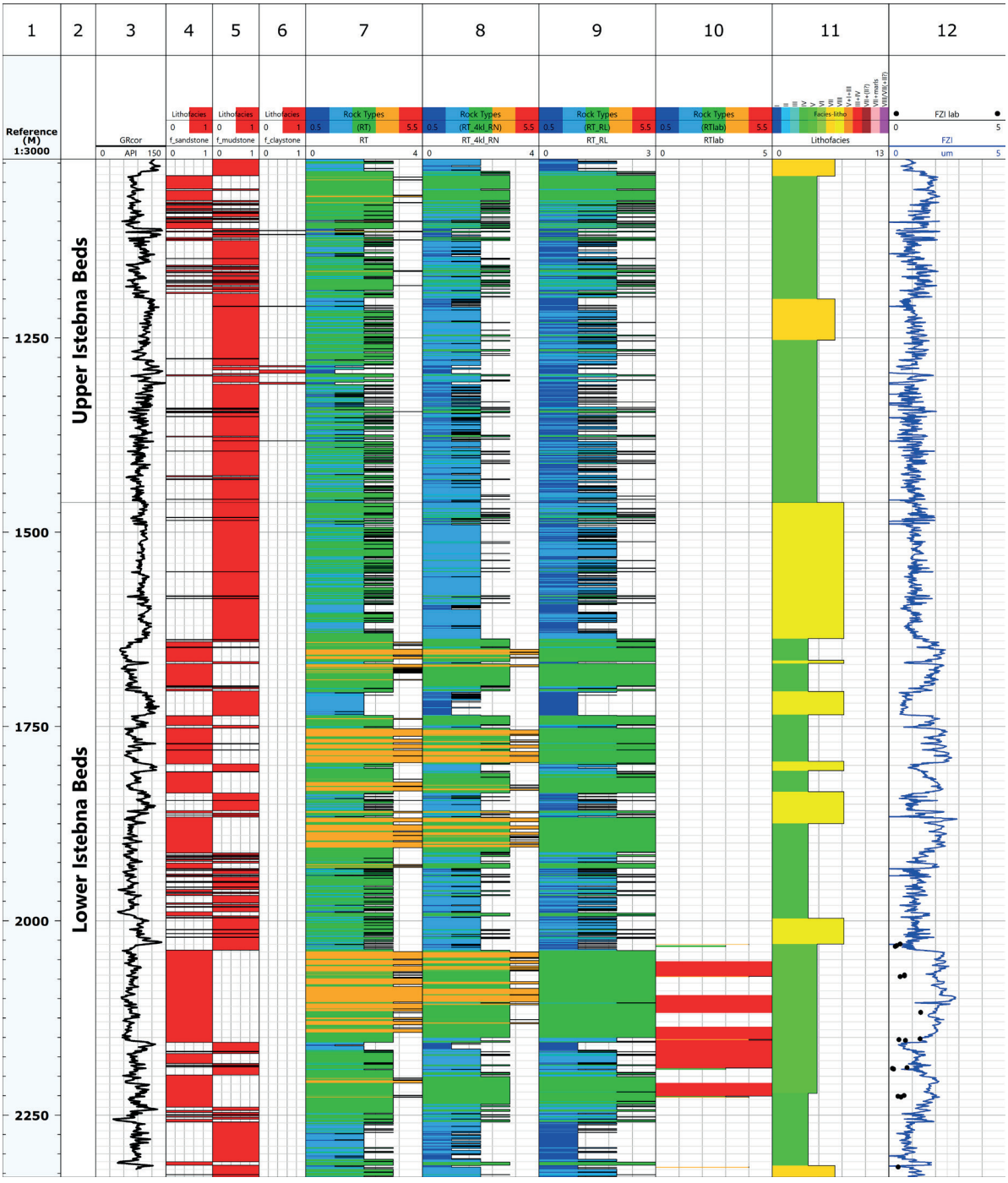

Fig. 6. *Facies separated in the profile of Istebna Beds in J-36 well, scale 1:3000. Description of paths: 1 – measured depth, 2 – lithostratigraphy, 3 – intensity of natural gamma-ray, 4, 5, 6 – petrophysical lithofacies on the basis of reinterpretation of well logging data, 7, 8, 9, – Rock Types separated on the basis of FZI subdivided according to Table 3, respectively, 10 – Rock Types separated from the FZI calculated on the basis of laboratory results (subdivision IV, Table 3), 11 – lithofacies determined on the basis of the descriptions of cores and cuttings, 12 – FZI and FZI_lab*

Based on the FZI subdivisions (Table 3), Rock Types (RT) were distinguished respectively to subdivision I, II and III (paths 7–9). On path 10 there is a facial division made based on FZI calculated from the laboratory results in the interval of the Istebna Beds (subdivision IV). Track 11 illustrates the lithofacies in the interval of the Istebna Beds on the basis of macroscopic descriptions of cores and cuttings included in the well documentation (Plezia 1995). The following lithofacies were distinguished, i.e. IV – coarse and medium-grained sandstones (dark blue), V – fine and medium-grained sandstones and shales (blue), VII – thin-bedded shales and sandstones (light blue) and VIII – shales and siltstones (green) (Fig. 6). In the Upper Istebna Beds, where the mudstone petrophysical lithofacies, f_mudstone, predominates the lithofacies V and VII were identified, while the Lower Istebna Beds are dominated by the lithofacies V, with VIII. The best reservoir capacity is shown by the Lower Istebna Beds in the interval of about 2038–2057 m, where sandstone lithofacies, f_sandstone, Rock Types for FZI of 2–4 and lithofacies V were determined. In a similar depth interval, the RT_lab parameter (path 10) was elaborated based on effective porosity and permeability determined from laboratory tests. The RT with the highest FZI dominates. The FZI values determined from laboratory data are included as dots on path 12, next to the continuous FZI curve. Lithofacies V and VII correlates with the high FZI values (path 12) and f_sandstone petrophysical lithofacies. Lithofacies VIII (with a high proportion of shale) clearly correlates with low FZI. The determined FZI values were lower on the basis of the laboratory data obtained from sandstones, nevertheless in the interval in which the laboratory tests were made facies with good reservoir properties are also evident.

Study material and results in M-6 well

The petrophysical lithofacies f_sandstone, f_mudstone and f_claystone were identified as in the previous well based on the results of well logging data reinterpretation. In the 11–2450 m interval of the M-6 well profile, the sandstone facies (f_sandstone) include about 29%, mudstone facies, f_mudstone about 68%, and claystone facies (f_claystone) about 3% of the profile. Throughout the entire profile of the well, the mudstone facies proved to be dominant. In the Istebna Beds (1905–2450 m interval), the sandstone facies accounted for about 34%, the mudstone about 64%, and the claystone about 2%. FZI was calculated based on the interpreted porosity (PHI) and the estimated permeability (K_{est}). The division into lithofacies is illustrated in Table 4. Similarly to the J-36 well, the division into sandstone horizons (A–E in Table 4) is marked based on the well documentation (Ratuszniak 1999).

The frequency distributions of FZI, divided into four classes (subdivision I, Table 3) are shown in Figure 7; for the whole profile (Fig. 7A) and for the Istebna Beds (Fig. 7B). The histograms are very similar, both in the whole profile and in the Istebna Beds FZI in the 0.5–1 class dominates. In the whole profile, this class accounts for more than 43%, while in the Istebna Beds for 45%. The percentages of FZI in classes smaller than 0.5 and 1 < FZI < 2 assume similar values and account for 26 and 30% in the entire profile and 26 and 28% in the Istebna Beds, respectively. A small number of measurements fall into the highest class 2–4 and FZI > 4.

The division into facies of the entire profile of the M-6 well was obtained by combining the results of various methods and is presented in Figure 8. The purpose was to highlight the dominance of the mudstone petrophysical lithofacies in the upper part of the profile and to show the facies differentiation between the Istebna Beds and other formations. Rock Types which are associated with FZI show the lowest values, i.e. FZI < 0.5 and 0.5 < FZI < 1 in the upper part of the profile. Only in the Ciężkowice Sandstones can a pronounced contribution of sandstone facies be seen. This is also evident in the form of green color for RT (1 < FZI < 2). There is a pronounced anomaly at the depth of about 475 m, where sandstone facies, Rock Types with values exceeding 4 and very high FZI values can be identified.

The same observation is true at the depth of 1825–1850 m, where there is a sequence of mudstone and sandstone facies characterized by high RT and high FZI values. At this depth, the lithofacies IV (coarse- to medium-grained sandstones) have been identified.

Table 4
Description of lithofacies separated in the Istebna Beds in the M-6 well based on descriptions of cores and cuttings

Lithostratigraphy (top and bottom) acc. to documentation	**Top [m]**	**Bottom [m]**	**Lithological division acc. to well data**	**No.**	**Lithofacies**
Upper Istebna Shales (1095–1150 m)	1095	1150	–	VII	thin-bedded shales and sandstones
Upper Istebna Sandstones (1150–1495 m)	1150	1184	sandstone, horizon A	III	thick-bedded conglomeratic sandstones
	1184	1189		VII	thin-bedded shales and sandstones
	1189	1237		III	thick-bedded conglomeratic sandstones
	1237	1244		VII	thin-bedded shales and sandstones
	1244	1277		III	thick-bedded conglomeratic sandstones
	1277	1312	grey shales with sandstone layers	II	paraconglomerates (debrites)
	1312	1345	sandstone, horizon B	V	fine- to medium-grained sandstones and shales
	1345	1406		II	paraconglomerates (debrites)
	1406	1495		V	fine- to medium-grained sandstones and shales
Lower Istebna Shales (1495–1700 m)	1495	1558	–	VIII	shales and mudstones
	1558	1700	–	VII	thin-bedded shales and sandstones
Lower Istebna Beds (1700–2450 m)	1700	1748	sandstone, horizon C1	IV	coarse- to medium-grained sandstones
	1748	1753	shales	VIII	shales and mudstones
	1753	1777	sandstone, horizon C2	V	fine- to medium-grained sandstones and shales
	1777	1803	shales	VII	thin-bedded shales and sandstones
	1803	1909	sandstone, horizon C3	IV	coarse- to medium-grained sandstones
	1909	1924	shales	VIII	shales and mudstones
	1924	1964	sandstone, horizon C4	IV	coarse- to medium-grained sandstones
	1964	2009	shales	VIII	shales and mudstones
	2009	2167	sandstone, horizon C5	IV	coarse- to medium-grained sandstones
	2167	2237	shales	VII	thin-bedded shales and sandstones
	2237	2336	sandstone, horizon D	V	fine- to medium-grained sandstones and shales
	2336	2354	shales	VIII	shales and mudstones
	2354	2450	sandstone, horizon E	V	fine- to medium-grained sandstones and shales

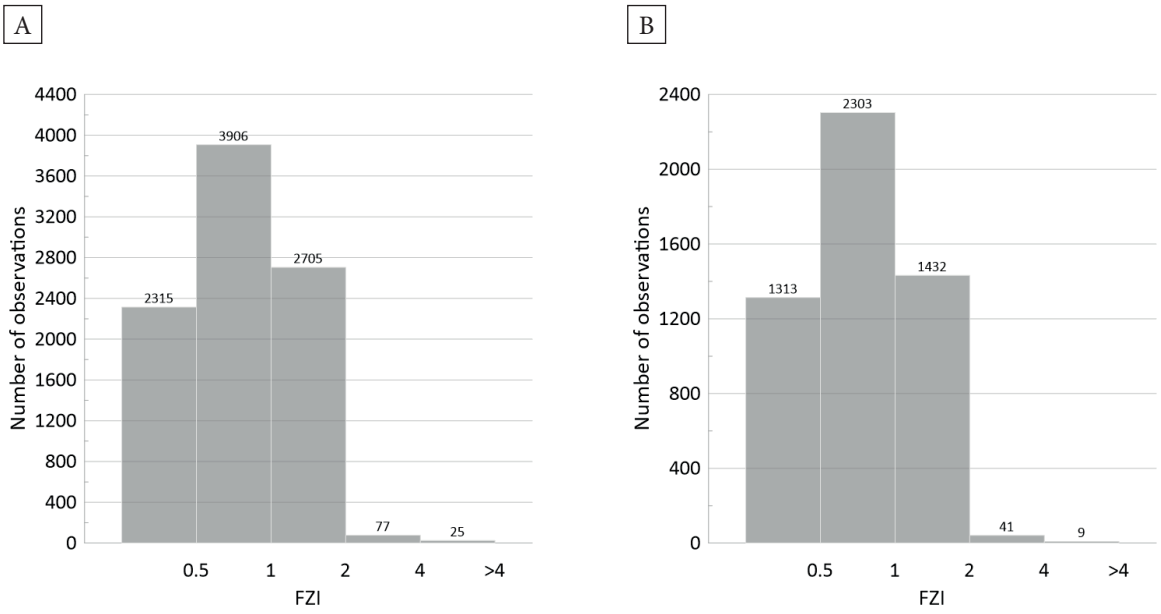

Fig. 7. *Histograms of FZI: A) in the entire profile of the M-6 well; B) in the Istebna Beds interval*

Noteworthy is the Lower Istebna Shale (1495–1700 m), where mudstone petrophysical lithofacies, low RT (navy blue) and lithofacies VII (shale and sandstone, thin-bedded) and VIII (shale and siltstone) are present. The Upper Istebna Shale (1095–1150 m, lithofacies VII) is characterized by similar RT results. The Upper Istebna Sandstones have significantly higher FZI values compared to the adjacent shale intervals. The sandstone-dominated lithofacies, i.e. II, III and V occur in this interval, showing increased flow capacity. In the Lower Istebna Beds, mudstone and sandstone facies are interspersed, as evidenced by RT (blue and green) and sandstone lithofacies IV and V, with thin insets of VII and VIII.

Discussion of the results obtained in the Istebna Beds in the Potok – Krościenko anticline area

A summary of the results in the Potok – Krościenko anticline, from the wells J-36, M-6 and So-29 and So-17 in the Istebna Beds, is illustrated in Figure 9. The facies similarity in the separated Upper and Lower Istebna Shales and Sandstones can be seen in all the wells. The base of the Istebna Beds in well So-29 and So-17 is at a greater depth compared to the J-36 and M-6 wells. In the J-36 and M-6 wells, a division is made into the Upper and Lower Istebna Shales, Upper Istebna Sandstones and Lower Istebna Beds. The intensity curve of natural radioactivity GR (path 3) shows elevated anomalies in the upper part of each profile (also in So-17 and So-29 wells), indicating the Upper Istebna Shales (occurred in J-36 and M-6). Similarly, an elevation in the GR curve indicating the Lower Istebna Shales is observed at a depth of about 1735–1845 m in the So-29 well and about 1750–1860 m in the So-17 well. The aforementioned intervals are in a mudstone facies, with a sandstone facies above and below.

These intervals exhibit RT in green, the most uniform green is in So-17, the greatest variation is in the M-6 well. The green color represents sections with $1 < FZI < 2$. In the Lower Istebna Beds, sandstone petrophysical lithofacies are much more abundant. The highest RT (FZI), i.e., the best media flow capacity is shown by the sandstones of the Lower Istebna Beds in the well So-29, moving westward along the Potok – Krościenko fold we observe facies with lower RT, where the lowest value is in the M-6 well. The lithofacies correlate with the RT divisions. A similarity in facies division is observed and the combined analysis of the various methods of facies differentiation allows for complementary information.

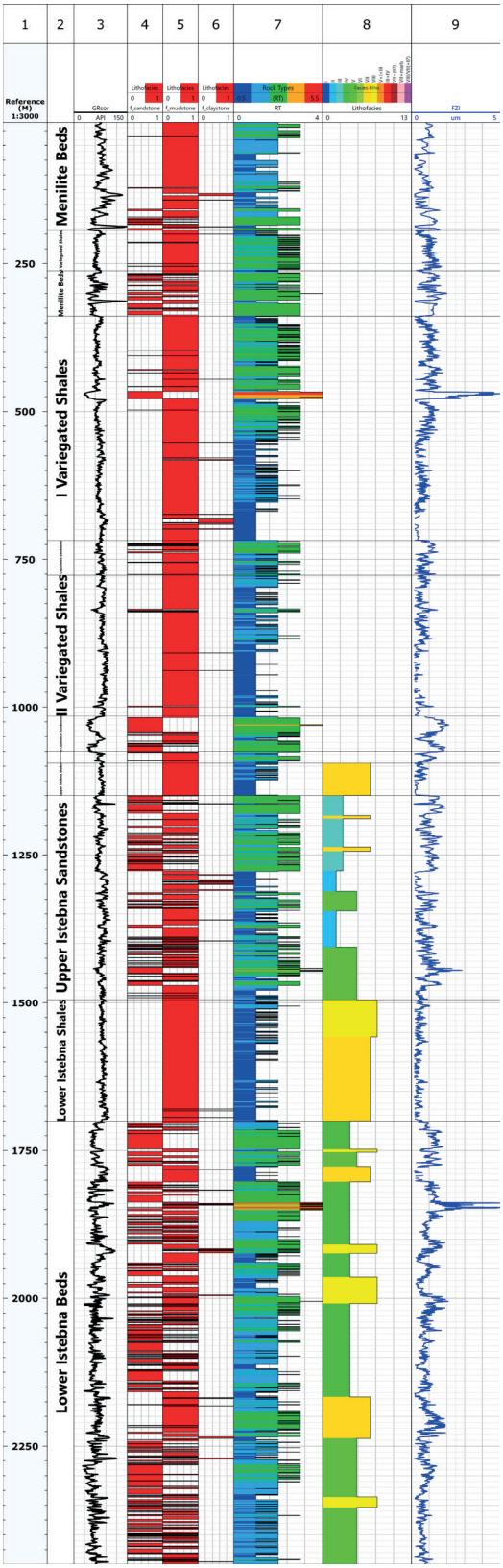

Fig. 8. *Division into facies on the basis of results of well logging data reinterpretation, Rock Types separated on the basis of FZI in the M-6 well profile and lithofacies separated on the basis of descriptions of cores and cuttings in the Istebna Beds, scale 1:3000. Description: 1 – measured depth, 2 – lithostratigraphy, 3 – intensity of natural gamma radioactivity, 4, 5, 6 – petrophysical lithofacies, 7 – Rock Types, 8 – lithofacies, 9 – FZI*

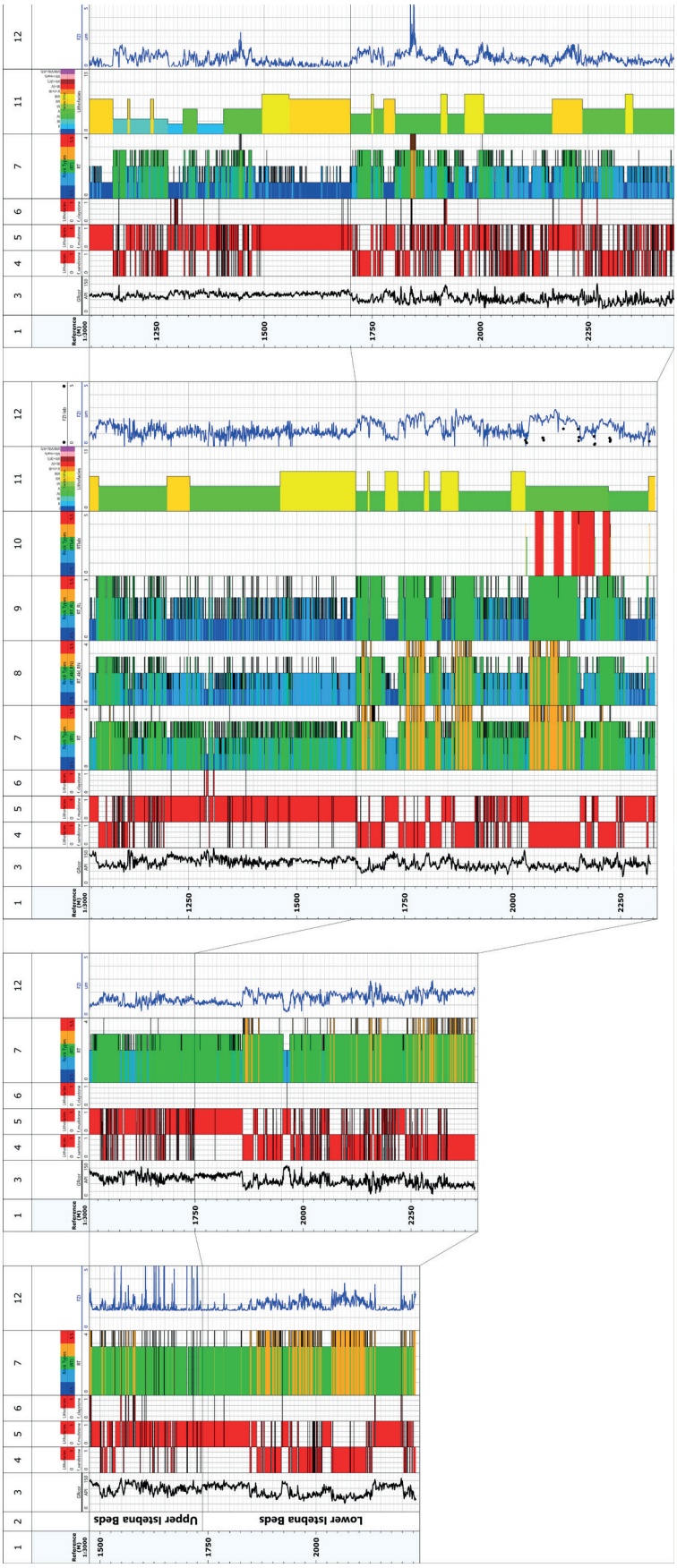

Fig. 9. *Facies distinguished in the Istebna Beds in So-29, So-17, J-36 and M-6 wells, scale 1:3000. Description: GRcor – gamma ray intensity, f_mudstone, f_sandstone, f_claystone – petrophysical lithofacies distinguished on the basis of the results of reinterpretation of well logging data, RT – Rock Types determined on the basis of FZI, lithofacies – determined according to the descriptions of cores and cuttings, FZI – Flow Zone Index*

Based on the presented facies analyses from various sources, it can be concluded that the formation of the Istebna Beds varies in both the J-36 and M-6 wells that are located in the axial zone of the Potok – Krościenko fold, and in the So-29 and So-17 wells located in its marginal part. This is evidence of the facies variability of the Istebna Beds along the stretch of the strata, manifested primarily by the different proportion (in terms of thickness and number of layers) of shale and/or debrite facies. In general, the Istebna Beds are characterized by a high degree of variation, both laterally and perpendicularly to the extension of the fold structure. This is especially true of the sandstone members (the Lower Istebna Beds and the Upper Istebna Sandstones), which build the main part of the profile of these lithostratigraphic unit. In both parts, the dominant facies are thick-bedded sandstones and conglomerates, but the individual packages do not form bodies of significant lateral extension but are lenticular in nature. This means that the profile of these strata observed at one location may differ significantly from that at another one, e.g. in terms of the ratio of sandstone to conglomerate facies, the different location in the profile of packets made up of conglomerate facies, the greater or lesser number and thickness of overlying packets of shale-sandstone facies, and above all, the different number and position in the profile of debrite intervals (lithofacies II). The latter are characterized by a lenticular structure and can pinch out over a relatively short distance – on the order of tens or even several meters. This variation is primarily due to the mode of deposition of the Istebna Beds, namely the sedimentation of their clastic material by gravity flows in a form of a slope apron (Strzeboński 2005, 2015). The lateral disappearance of some facies and the appearance of others in different areas along the extension of individual folds is the reason for the variable character of the Istebna Beds in the study area. Individual facies are repeated many times in the profile of these Beds, but as the facies are characterized by lateral discontinuity, differences in their lithological character (i.e., variations in the succession and contribution of individual facies to the vertical profile) can be expected even in neighboring wells.

MAPS OF RESERVOIR PARAMETERS OF THE ISTEBNA BEDS IN THE STUDY AREA

The maps were prepared using reservoir parameters, i.e. porosity (PHI), permeability (*K*) and the coefficient defining the ability of rocks to media flow (FZI) calculated based on the results of the reinterpretation of well logging (Stadmüller et al. 2021–2022). The Istebna Beds were divided in two ways: distinguishing the Istebna Upper and Lower Beds (division into two parts) and distinguishing the Istebna Upper Sandstone and Shale, the Istebna Lower Shale, and the Istebna Lower Beds (a division into three parts). In the first division, the Upper Istebna Beds included Paleocene formations or Paleocene and Upper Cretaceous formations, while the Lower Istebna Beds included Upper Cretaceous formations. In the second division, in most of the well profiles analyzed, the Lower Istebna Shales were of Upper Cretaceous age but, for example, in the So-17 well they were of Paleocene age.

Maps of the values of physical permeability, effective porosity, and coefficient FZI were made using the Petrel Schlumberger software based on the data entered at the points described by the coordinates of the wells. The minimum, maximum, and arithmetic mean values of all parameters were calculated, as well as the depths of the top and bottom of the lithostratigraphic units. The maps illustrate the average values of the parameters, assigned to the average depths of the lithostratigraphic units (Table 5). The data on the basis of which the maps were prepared came from 16 wells: B-1A, Dr-1, Dr-4k, Du-1, J-24, J-32A, J-35, J-36, Kr-4k, M-6, Os-138, Si-1, So-17, So-29, R-1, R-2. The location of these wells is shown on the background of the geological map (Fig. 10). The version of the map does not include tectonic features interpreted from seismic data. In Figure 10 the full names of the wells are written while the wells are described by abbreviated names in later figures.

Physical permeability was estimated based on effective porosity. Thus, very high values of *K* (about 144 mD), that appeared in profiles of some wells, such as Os-138 well, were associated with high values of the effective porosity (>20%).

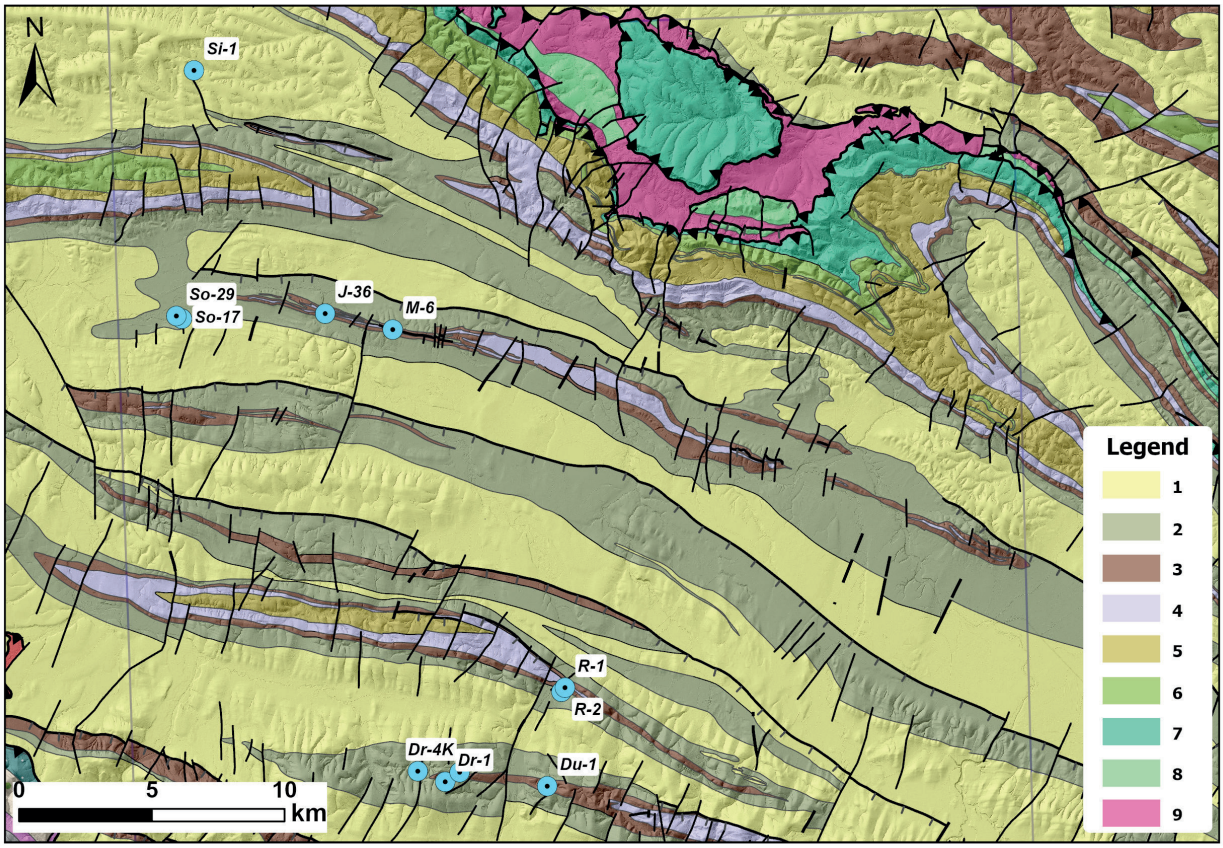

Fig. 10. *Distribution of the selected wells on the background of the geological map roughly illustrating the area where the K, PHI and FZI maps were made. Explanations: 1, 2 – Krosno Beds (1 – sandstones and shales, 2 – thick-bedded sandstones), 3 – Menilite Beds, 4 – Hieroglyphic Beds, Variegated Shales and Ciężkowice Sandstones, 5, 6 – Istebna Beds (5 – Upper, 6 – Lower), 7 – Lower Cretaceous formations of the Silesian Unit, 8 – Lower and Upper Cretaceous formations of the Sub-Silesian Unit, 9 – Variegated Marls of the Sub-Silesian Unit (map acc. to Szymakowska & Wójcik 1981, Piotrowska & Wasiluk 2009a, 2009b, Starzec 2016)*

Under the assumption that the porosity of the Istebna Beds does not exceed 20% (supported by results in neighboring wells and laboratory results), the values of physical permeability did not exceed about 70 mD. Porosity and permeability values were also constrained from below with the lowest porosities higher than 0.001 and permeabilities higher than 0.001 mD. Very low porosities and permeabilities generated anomalously high FZI values. The average values of all parameters calculated with and after removing the extreme values did not differ significantly, which means that the number of extreme values was not large.

As an example of the data on which the maps were based, i.e. the average values of the FZI, PHI and *K* parameters for the upper and lower interval of the Istebna Beds is shown in Table 5. The average values appearing in Table 5 were calculated without considering extreme values.

The maps of average FZI values for the Upper Istebna Beds are shown in Figure 11. The different results for the Istebna Beds divided into two- and three-parts are illustrated. The impact of extremely high values is also shown, which can be counted as interpretive errors. To highlight the additional information obtained with the division of the Istebna Beds into three parts, Figure 12 shows a map of the average *K* and FZI values for the Lower Istebna Shale, to emphasize that the separation of these shales allows highlighting the levels with higher flow capacity.

Table 5
Mean values of FZI, PHI and K parameters in the Upper and Lower Istebna Beds

Well	Upper Istebna Beds			Lower Istebna Beds		
	Parameter			Parameter		
	FZI [μm]	**PHI [dec]**	***K* [mD]**	**FZI [μm]**	**PHI [dec]**	***K* [mD]**
O-138	2.274	0.110	12.898	1.977	0.118	12.791
R-2	3.288	0.057	2.374	3.429	0.051	1.842
R-1	1.350	0.059	0.812	2.180	0.037	0.082
K-4k	0.727	0.057	0.820	–		
M-6	0.706	0.045	0.486	0.897	0.058	1.011
S-29	1.854	0.040	0.040	2.015	0.065	2.190
S-17	0.424	0.059	0.601	1.601	0.071	1.807
D-4K	1.131	0.031	0.591	–		
Du-1	2.243	0.044	1.853	2.292	0.040	0.912
J-36	1.129	0.053	0.612	1.555	0.069	2.907
Si-1	1.352	0.038	0.653	1.342	0.034	0.570
D-1	2.155	0.024	0.824	2.224	0.021	1.158
J-35	1.147	0.052	0.710	1.444	0.064	1.972
J-32A	1.049	0.042	0.322	1.553	0.069	2.804
J-24	1.187	0.048	0.693	1.552	0.070	2.679
B-1A	1.830	0.027	0.111	1.876	0.028	0.084

The distribution of petrophysical parameters is depicted on the geological map to illustrate their relation to geological structures in the study area (Fig. 13). Well Si-1, the northernmost in the group of studied wells, is located on the axial zone of the Glinik syncline. Well So- 29 and So-17, J-36 and M-6 are located on the Potok – Krościenko anticline. Well R-1 and R-2 were drilled within the Bóbrka – Rogi anticline. Wells Dr-1, Dr-2 and Dr-4K and Du-1 were situated in the axial zone of the Iwonicz-Zdrój – Draganowa anticline (Fig. 10). Well Os-138 is located on the central-western part of the study area, and well B-1A is located in the central-eastern part. The anomalies observed in the *K*, PHI and FZI maps are related to geological structures.

The link between the distribution of FZI and geological structures is manifested in the tendency of the value of this parameter to decrease towards the NNE, i.e. towards the marginal zone of the Silesian Unit. The southern folds: Iwonicz-Zdrój – Draganowa and Bóbrka – Rogi, and further to the west also the Osobnica fold are characterized by higher values of FZI, while structural elements occurring more to the north are characterized by lower values, in general FZI distribution shows a belt arrangement, more or less relating to the belt pattern of the folds. Such a pattern is visible in case of both the Lower and Upper Istebna Beds, although two anomalies can be observed in the Upper Istebna Beds (Fig. 13): 1) a distinct extension to the SW of the low values in the region of Kr-4k well (the region indicated by the orange arrow): this shape refers to the curved shape of the front of the Silesian Unit, evidencing that the values are related to the tectonic structures of the area; 2) the low-value anomaly perpendicular to the extension of the folds (black arrow) that most probably are related to the disappearance of the Iwonicz-Zdrój – Draganowa fold in this area that further to the west probably does not continue. The geological situation in the case of the Bóbrka – Rogi fold is different, because this fold plunges towards the west and it disappears at the surface, but then again, the axis of the fold is tilted upwards and continues as the Osobnica fold. In the case of the Lower Istebna Beds, this type of anomaly does not occur, but the strip pattern of the FZI, generally referring to the fold pattern, is preserved.

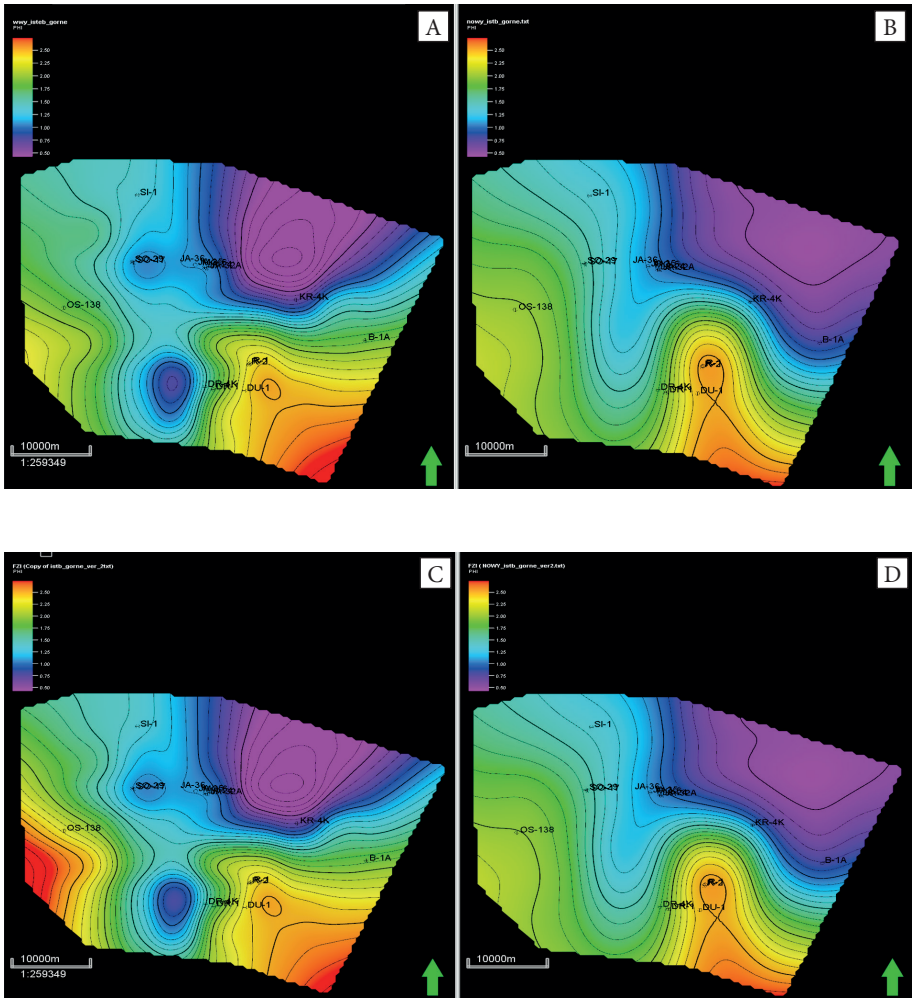

Fig. 11. Maps of average FZI values in the Upper Istebna Beds; the maps A and B were created based on all values estimated as a result of reinterpretation of well logging, the maps C and D represent the values after reduction of the highest permeabilities; A and C maps – division into two parts, B and D maps – division into three parts

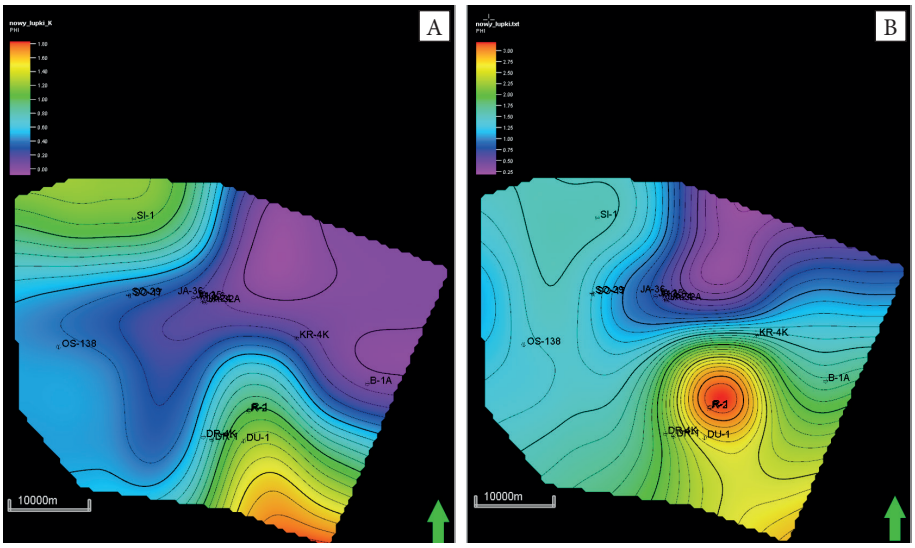

Fig. 12. Maps of average values of permeability K (A) and FZI (B) in the Lower Istebna Shale (values after reduction of extreme results); divided into three parts

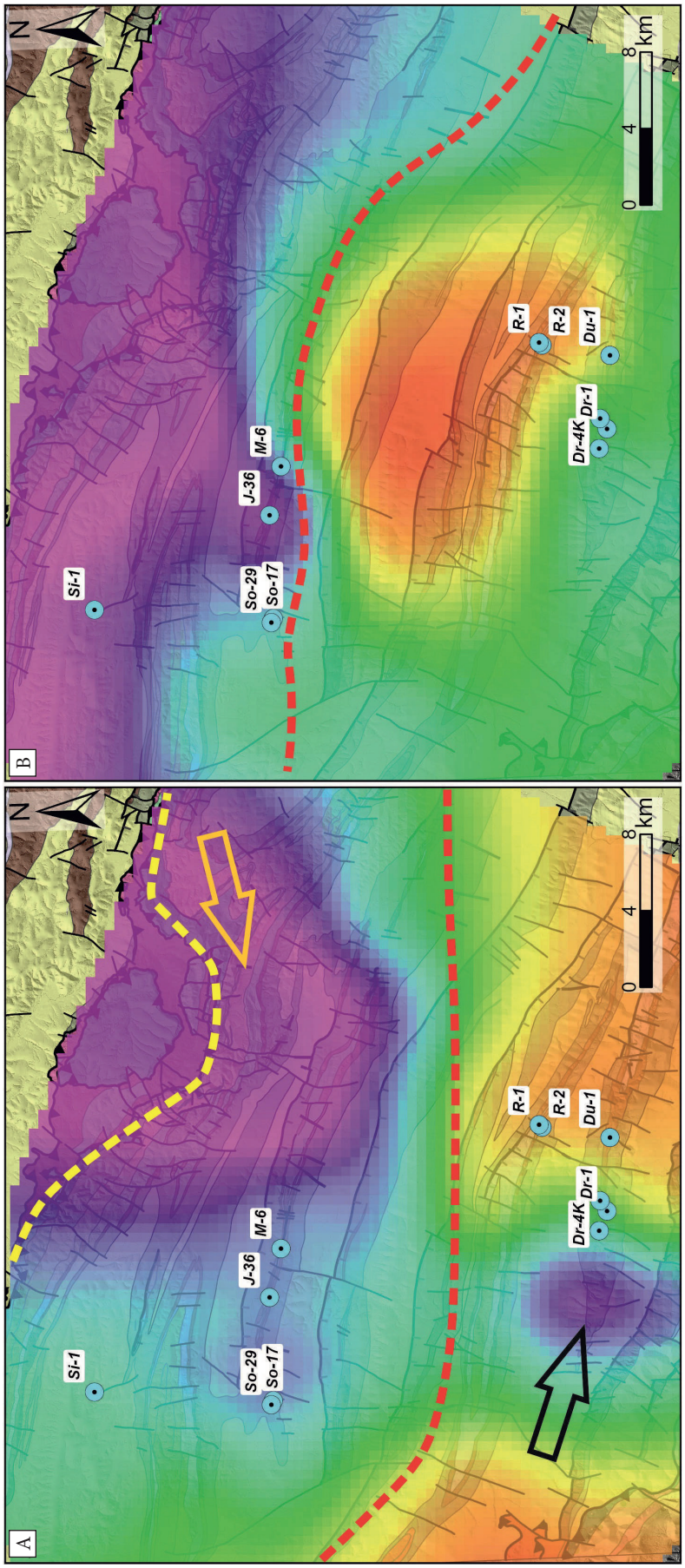

Fig. 13. *FZI in the Upper (A) and Lower (B) Istebna Beds (division into three parts); yellow line – front of the Silesian Unit overlap, red line – separates the southern zone of the Silesian Unit with higher FZI values from the northern zone with lower values; purple – lowest values, red – highest values*

DISCUSSION

Manual interpretation of well logging in terms of determining lithology, porosity, and saturation not only consumes a lot of time, but is also not free of human error. In recent years, geosciences have witnessed significant advancements in AI technology, notably in automating tasks such as velocity inversion (Yang & Ma 2019), seismic facies analysis (Nasim et al. 2022) or lithology prediction (Meshalkin et al. 2020). Increasingly, the algorithms used for machine recognition of lithology using well logging are based directly on well logs (Alzubaidi et al. 2021, Jiang et al. 2021). 3D petrophysical and temperature models provide necessary information on storage potential, transport properties, and temperature conditions in geothermal reservoirs, so the facies division from well logging interpretation is very useful (Slota-Valim et al. 2024). Machine learning (ML) tools shed light on the recognition and characterization of petroleum and geothermal systems using well log data as a source of porosity and permeability (parallel with laboratory results). An important feature of ML algorithms is their capability to synthesize high-dimensional data and find hidden interactions (Topór & Sowiżdżał 2023).

A novelty in the presented work is utilizing FZI, a quantity that performs a combined projection of the reservoir capacity of the rock. In the presented case, continuous FZI curves and pointwise but direct geological information increase the chances of correct facies differentiation. Continuous FZI curves can also be directly incorporated into machine learning methods alongside well logs.

Distinguishing geological lithofacies in different parts of the profile of the Istebna Beds allows for a consideration of the individual characteristics of sandstones and shales. Showing them against the background of a continuous Rock Types subdivision makes it possible to incorporate individual geological features, such as grain size or layering pattern, into an overall continuous characterization. The analysis of Rock Types with the incorporation of lithofacies and lithofacies allows us to divide the continuous profile of the Istebna Beds into smaller fragments with similar properties. This patchwork approach is also used in algorithms for the automatic identification of facies (Alaudah et al. 2019) allowing for an increase in the amount of data. It is also worth noting that researchers using machine learning algorithms and comparative analysis employ the volume of shale derived from the shaliness index as an important element for distinguishing lithologies (Kumar et al. 2022). The procedure for separating the petrophysical lithofacies used in this work is also based directly on shaliness.

CONCLUSIONS

The presented results have shown that the integration of data acquired from different sources, with various scales of accuracy, makes it possible to enrich and refine geological information. An important effect is the integration of geological information obtained directly from outcrops at the macro scale into the detailed considerations made possible based on well logging data. It is also important to emphasize the compatibility of micro-scale laboratory data and meso-scale well logging data. The continuous information on FZI and Rock Types determined on the basis of this parameter complements the lithological data. The unique combination of porosity and permeability in the FZI is a distinctive extension of the rock description.

The analyses of reservoir parameters based on the FZI and the Rock Types, as well as the lithology-based facies divisions, i.e. petrophysical lithofacies based on the results of the well logging interpretation and lithofacies based on the results of the field survey combined with the description of cores and cuttings, allowed us to conclude that the Lower Istebna Beds are characterized by the best flow capacity and lithofacies with the highest sandstone content. It is also worth noting that the applied divisions into four or three Rock Types give more detailed information compared to the division into petrophysical lithofacies alone: f_sandstone, f_mudstone and f_claystone. The extracted Rock Types also agree with the lithofacies determined solely on the basis of macroscopic features. The calculation of Rock Types is an extension of the information provided by the well logging interpretation and can facilitate the decision

on possible perforation of selected sections of the profile.

The maps of reservoir parameters, porosity, permeability and flow coefficient, when compared with geological maps, confirm the connection between their distribution and geological structures. The analysis presented for the Istebna Beds is a model algorithm that can be applied to other formations when selecting the best sections of the geological profile in terms of the reservoir characteristics studied for the prospection of hydrocarbons and water – whether for potable or geothermal purposes.

The results were obtained as part of the "Development of an innovative concept for searching for hydrocarbon deposits in the deep structures of the Outer Carpathians", INNKARP (2019–2023) project, co-executed by AGH University of Krakow, Poland, financed in the framework of the Smart Growth Operational Programme by the National Center for Research and Development and PGNiG S.A., Warsaw, Poland. The article was also partially funded by the Ministry of Science and Higher Education in Poland subsidy 16.16.140.315 for the Faculty of Geology, Geophysics, and Environmental Protection of the AGH University of Krakow.

The Authors would like to thank POGC S.A. for sharing their data sharing and their gratitude is also extended to Dr. Monika Kasperska and Dr. Anita Lis-Śledziona for their contributions. The Techlog and Petrel software were used thanks to Slb as a university program for AGH University of Krakow.

Author contributions: *P.I.K.-M.: concept of research work and article structure, investigations, methodology, petrophysical interpretation, graphical side of the paper, edition; E.P.: concept of research work, investigation, methodology, petrophysical interpretation; K.S.: field geological investigations, lithofacies definitions and descriptions, geological interpretation; J.A.J.: concept of article, project administration, supervision, writing original draft; M.S.: well logging interpretation, methodology.*

All of the authors have read and agreed to the published version of the manuscript.

REFERENCES

Al-Askari G. & Kamal M., 2017. Methods for determination of hydraulic flow units using petrophysical parameters (case study from South Pars Gas Field, Iran). *International Journal of Progressive Sciences and Technologies*, 6(1), 73–83.

Al-Jawad S.N. & Saleh A.H., 2020. Flow units and rock type for reservoir characterization in carbonate reservoir: case study, south of Iraq. *Journal of Petroleum Exploration and Production Technology*, 10, 1–20. https://doi.org/10.1007/s13202-019-0736-4.

Alaudah Y., Michałowicz P., Alfarraj M. & Alregib G., 2019. A machine-learning benchmark for facies classification. *Interpretation*, 7(3), 1–51. https://doi.org/10.1190/INT-2018-0249.1.

Alberty M. & Hashmy K.H., 1984. *Application of ULTRA to log analysis* [conference paper]. SPWLA 25th Annual Logging Symposium, New Orleans, Louisiana, June 1984, SPWLA-1984-Z.

Alzubaidi F., Mostaghimi P., Swietojanski P., Clark S.R. & Armstrong R.T., 2021. Automated lithology classification from drill core images using convolutional neural networks. *Journal of Petroleum Science and Engineering*, 197, 107933. https://doi.org/10.1016/j.petrol.2020.107933.

Amaefule J.O., Altunbay M., Tiab D., Kersey D.G. & Keeland D.K., 1993. *Enhanced reservoir description: using core and log data to identify hydraulic (flow) units and predict permeability in uncored intervals/wells* [conference paper]. SPE Annual Technical Conference and Exhibition, Houston, Texas, October 1993, SPE-26436-MS. https://doi.org/10.2118/26436-MS.

Baszkiewicz A., Dziadzio P. & Probulski J., 2001. Stratygrafia sekwencji, petrogeneza i potencjał zbiornikowy piaskowców istebniańskich i ciężkowickich w zachodniej części fałdu Iwonicza Zdroju. *Przegląd Geologiczny*, 49(5), 417–424.

Birkenmajer-Szymakowska F., Jasionowicz J. & Wójcik A., 2009. *Szczegółowa mapa geologiczna Polski 1:50 000, arkusz Frysztak (1003)* [tectonic and geological sketch]. Narodowe Archiwum Geologiczne PIG-PIB, Warszawa.

Doveton J.H. & Prensky S.E., 1992. Geological applications of wireline logs – a synopsis of developments and trends. *The Log Analyst*, 33(3), 286–302.

Dziadzio P.S., 2006. The geology of the Weglowka oil field, Subsilesian unit, Polish Outer Carpathians. [in:] Golonka J. & Picha F.J. (eds.), *The Carpathians and their foreland: Geology and hydrocarbon resources*, AAPG Memoir, 84, American Association of Petroleum Geologists, Tulsa, 467–476. https://doi.org/10.1306/985616M843071.

Houshmand N., GoodFellow S., Esmaeili K. & Ordóñez Calderón J.C., 2022. Rock type classification based on petrophysical, geochemical, and core imaging data using machine and deep learning techniques. *Applied Computing and Geosciences*, 16, 100104. https://doi.org/10.1016/j.acags.2022.100104.

Jankowski L., Kopciowski R. & Ryłko W., 2012. Stan wiedzy o budowie geologicznej Karpat zewnętrznych pomiędzy rzekami Białą a Risca – dyskusja. *Biuletyn Państwowego Instytutu Geologicznego*, 449, 203–216.

Jarzyna J., Bała M., Cichy A., Karczewski J., Zorski T., Twaróg W., Gądek W., Stadtmüller M., Gąsior I. & Marzencki K., 2000. System GeoWin w środowisku Windows – programy do przetwarzania i interpretacji profilowań geofizyki wiertniczej. *Prace Instytutu Górnictwa Naftowego i Gazownictwa*, 110, 253–257.

Jarzyna J., Puskarczyk E., Krakowska P., Wawrzyniak-Guz K., Kasperska M., Waszkiewicz S. & Wilkosz M., 2021–2022. Task 2 in the project *Opracowanie innowacyjnej koncepcji poszukiwania złóż węglowodorów w głębokich strukturach Karpat Zewnętrznych (INNKARP)* co-implemented by AGH University of Krakow in 2019–2022, funded by National Centre for Research and Development and Polish Oil and Gas Company within the funds „Inteligentny Rozwój 2014–2020". Archive of Department of Geophysics, Faculty of Geology, Geophysics and Environmental Protection, AGH University of Krakow [unpublished].

Jiang C., Zhang D. & Chen S., 2021. Lithology identification from well log curves via neural networks with additional geological constraint. *Geophysics*, 86(5), 1–77. https://doi.org/10.1190/geo2020-0676.1.

Kępińska B., 1986. Podział utworów górnej kredy i paleocenu centralnej części fałdu Brzanka-Liwocz (jednostka śląska). *Geological Quarterly*, 30, 63–76.

Konarski E., 1980. *Wgłębna budowa karpackiej pokrywy fliszowej w rejonie gorlicko-krośnieńskim*. Wydawnictwa Geologiczne, Warszawa.

Kruczek J., 1956. Geologia antykliny Łężyny – Świerchowa. *Biuletyn Instytutu Geologicznego*, 110, 139–197.

Kruczek J., 1968. Strukturalne ramy akumulacji ropy w złożu Bóbrka-Rogi. *Biuletyn Instytutu Geologicznego*, 215, 79–137.

Kruczek J., 1999. *Aktualne rozpoznanie tektoniki fliszu Karpackiego w rejonie Sanok – Krosno – Gorlice*. Prace Instytutu G*órnictwa* Naftowego i Gazownictwa, 98, Instytut Górnictwa Naftowego i Gazownictwa, Kraków.

Książkiewicz M., 1977. The tectonics of the Carpathians. [in:] Pożaryski W. (ed.), *Tectonics*, Geology of Poland, 4, Wydawnictwa Geologiczne, Warszawa, 476–620.

Kumar T., Seelam N.K. & Rao G.S., 2022. Lithology prediction from well log data using machine learning techniques: A case study from Talcher coalfield, Eastern India. *Journal of Applied Geophysics*, 199, 104605. https://doi.org/10.1016/j.jappgeo.2022.104605.

Mahjour S.K., Kamal M., Al-Askari G. & Masihi M., 2015. Identification of flow-units using methods of Testerman statistical zonation, flow zone index, and cluster analysis in Tabnaak gas field. *Journal of Petroleum & Environmental Biotechnology*, 6(6), 253. https://doi.org/10.4172/2157-7463.1000253.

Mahmoud A.I., Metwally A.M., Mabrouk W.M. & Leila M., 2023. Controls on hydrocarbon accumulation in the prerift Paleozoic and late syn-rift Cretaceous sandstones in PTAH oil field, north Western Desert, Egypt: Insights from seismic stratigraphy, petrophysical rock-typing and organic geochemistry. *Marine and Petroleum Geology*, 155, 106398. https://doi.org/10.1016/j.marpetgeo.2023.106398.

Meshalkin Y., Shakirov A., Orlov D. & Koroteev D., 2020. *Well-logging based lithology prediction using machine learning*. EarthDoc, Data Science in Oil and Gas, European Association of Geoscientists & Engineers. https://doi.org/10.3997/2214-4609.202054010.

Mitura F. & Birecki T., 1966. *Budowa geologiczna Karpat między Korczyną a Domaradzem*. Prace Instytutu Naftowego, 90, Wydawnictwo „Śląsk", Katowice.

Nasim M.Q., Maiti T., Srivastava A., Singh T. & Mei J., 2022. Seismic Facies Analysis: A Deep Domain Adaptation Approach. *IEEE Transactions on Geoscience and Remote Sensing*, 60, 4508116. https://doi.org/10.1109/TGRS.2022.3151883.

Oszczypko N., Ślączka A. & Żytko K., 2008. Regionalizacja tektoniczna Polski – Karpaty zewnętrzne i zapadlisko przedkarpackie. *Przegląd Geologiczny*, 56(10), 927–935.

Paul Z., Ryłko W. & Tomaś A., 1996. Zarys budowy geologicznej zachodniej części Karpat polskich (bez utworów czwartorzędowych). *Przegląd Geologiczny*, 44(5), 469–475.

Piotrowska K. & Wasiluk R., 2009a. *Szczegółowa mapa geologiczna Polski 1:25 000, arkusz Krosno (1023)* [tectonic and geological sketch]. Państwowy Instytut Geologiczny – Państwowy Instytut Badawczy, Warszawa.

Piotrowska K. & Wasiluk R., 2009b. *Objaśnienia do Szczegółowej mapy geologicznej Polski 1:50 000, arkusz Krosno (1023)*. Państwowy Instytut Geologiczny – Państwowy Instytut Badawczy, Warszawa.

Plezia B., 1995. *Dokumentacja wynikowa odwiertu rozpoznawczego Jaszczew-36*. PGNiG, Warszawa [unpublished].

Prasad M., 1999. Correlating permeability with velocity using flow zone indicators. *SEG Technical Program Expanded Abstracts*, 18(1), 184–187. https://doi.org/10.1190/1.1820904.

Prasad M., 2003. Velocity-permeability relations within hydraulic units. *Geophysics*, 68(1), 108–117. https://doi.org/10.1190/1.1543198.

Ratuszniak Z., 1999. *Dokumentacja wynikowa pogłębionego otworu Moderówka-6*. PGNiG SA, Oddział BG GEONAFTA, Warszawa [unpublished].

Saadat K. & Rahimpour-Bonab H., 2023. Lithology determination and petrophysical rock typing of sedimentary rocks using X-ray tomography. *Geoenergy Science and Engineering*, 231(part B), 212397. https://doi.org/10.1016/j.geoen.2023.212397.

Słota-Valim M., Lis-Śledziona A. & Topór T., 2024. Geothermal energy potential of Main Dolomite formation in SW Poland. *Geology, Geophysics & Environment*, 50(3), 275–293. https://doi.org/10.7494/geol.2024.50.4.275.

Stadtmüller M., Lis-Śledziona A. & Kubik B., 2021–2022. Dokumentacja projektu *Opracowanie innowacyjnej koncepcji poszukiwania złóż węglowodorów w głębokich strukturach Karpat Zewnętrznych*. INKARP nr POIR.04.01.01-00-0006/18-00 Etap I, Archive of INiG-PIB, Krakow [unpublished].

Stadtmüller M., Lis-Śledziona A., Krakowska-Madejska P. & Jarzyna J., 2022. Charakterystyka jednostek geologicznych na podstawie geofizyki wiertniczej i danych geologicznych, przykłady z jednostki śląskiej, z polskich Karpat Zewnętrznych. [in:] *Geopetrol 2022: Wyzwania dla sektora naftowego i gazowniczego w dobie transformacji energetycznej: Międzynarodowa Konferencja Naukowo-Techniczna: [19–21 września 2022, Zakopane]: materiały konferencyjne*, Instytut Nafty i Gazu – Państwowy Instytut Badawczy, Kraków, 359–372.

Starzec K., 2016. *Opracowanie powierzchniowej mapy geologicznej dla obszaru koncesji Sobniów – Kombornia – Rogi na podstawie materiałów archiwalnych pod kątem identyfikacji elementów składowych procesów generowania, migracji i akumulacji węglowodorów*. Program Blue Gas II Projekt ShaleCarp, Archive of AGH University of Krakow [unpublished].

Strzeboński P., 2005. Debryty kohezyjne warstw istebniańskich (senon górny – paleocen) na zachód od Skawy. *Geologia – Akademia Górniczo-Hutnicza im. Stanisława Staszica w Krakowie*, 31(2), 201–224.

Strzeboński P., 2015. Late Cretaceous-Early Paleogene sandy-to-gravelly debris flows and their sediments in the Silesian Basin of the Alpine Tethys (Western Outer Carpathians, Istebna Formation). *Geological Quarterly*, 59(1), 195–214. https://doi.org/10.7306/gq.1183.

Szymakowska F. & Wójcik A., 1981. *Szczegółowa mapa geologiczna Polski 1:50 000, arkusz Jedlicze*. Instytut Geologiczny, Warszawa.

Szymakowska F. & Wójcik A., 1992a. *Szczegółowa mapa geologiczna Polski 1:50 000, arkusz Jedlicze* [tectonic and geological sketch]. Instytut Geologiczny, Warszawa.

Szymakowska F. & Wójcik A., 1992b. *Objaśnienia do Szczegółowej mapy geologicznej Polski 1:50 000, arkusz Jedlicze*. Instytut Geologiczny, Warszawa.

Topór T. & Sowiżdżał K., 2023. An advanced ensemble modeling approach for predicting carbonate reservoir porosity from seismic attributes. *Geology, Geophysics & Environment*, 49(3), 245–260. https://doi.org/10.7494/geol.2023.49.3.245.

Unrug R., 1963. Istebna beds – a fluxoturbidity formation in the Carpathian Flysch. *Rocznik Polskiego Towarzystwa Geologicznego*, 33(1), 49–92.

Wdowiarz J., 1950. Zdjęcie geologiczne fałdów Iwonicza–Klimkówki–Rymanowa. *Rocznik Polskiego Towarzystwa Geologicznego*, 19, 435–444.

Wdowiarz S., Zubrzycki A. & Frysztak-Wołkowska A., 1991a. *Szczegółowa mapa geologiczna Polski 1:50 000, arkusz Rymanów* [tectonic and geological sketch]. Instytut Geologiczny, Warszawa.

Wdowiarz S., Zubrzycki A. & Frysztak-Wołkowska A., 1991b. *Objaśnienia do Szczegółowej mapy geologicznej Polski 1:50 000, arkusz Rymanów*. Instytut Geologiczny, Warszawa.

Yang F. & Ma J., 2019. Deep-learning inversion: A next-generation seismic velocity model building method. *Geophysics*, 84(4), R583–R599. https://doi.org/10.1190/geo2018-0249.1.

Zawisza L., 1993. Simplified method of absolute permeability estimation of porous beds. *Archives of Mining Sciences*, 38(4), 343–352.